

Multiphoton Isotope-Selective Dissociation of Formic Acid Molecules under Action of a Free Electron Laser

Alexander K. Petrov, Evgeni N. Chesnokov, Sergey R. Gorelik, Karl D. Straub,*
Eric B. Szarmes, and John M. J. Madey

Institute of Chemical Kinetics and Combustion, Novosibirsk, 630090, Russia, and Free Electron Laser Laboratory, Duke University, Durham, North Carolina 27708-0319

Received: March 20, 1997; In Final Form: June 20, 1997[⊗]

The infrared multiphoton dissociation (IR MPD) of formic acid molecules ($\text{HCOOH} \rightarrow \text{CO} + \text{H}_2\text{O}$) with free electron laser radiation in the $3 \mu\text{m}$ region (C–H stretch vibrational absorption band) and in the $6 \mu\text{m}$ region (C=O stretch vibrational absorption band) has been achieved using the same laser. Results indicate that initial excitation of this dimer is more efficient for MPD than initial monomer excitation. Carbon isotope-selective MPD has been performed with an isotopic mixture, $\text{H}^{12}\text{COOH} + \text{H}^{13}\text{COOH}$ (50% + 50%), at an irradiating wavelength of $5.56 \mu\text{m}$. For this mixture, isotopic selectivity $s = k_{12}/k_{13} = 23$ has been attained as a ratio of the rate constants of the H^{12}COOH MPD and the H^{13}COOH MPD, respectively. The isotopic selectivity for ^{13}C in the naturally occurring mixture (1.1% of ^{13}C -containing molecules) $s = k_{13}/k_{12} = 22$ has been attained at an irradiating wavelength of $5.90 \mu\text{m}$.

Introduction

A very large body of experimental and theoretical work on infrared multiphoton dissociation (MPD) has been accomplished since such reactions were first described over 20 years ago.^{1–4} Of that work, a substantial proportion is concerned with isotope-specific MPD.^{5–29} Isotopic enrichment in the gas phase of small molecules has been accomplished for sulfur,^{6–9} oxygen,^{10–13} hydrogen,^{14–18} silicon²⁴ and multiple elements from the same compound.^{19–23} The most extensive work has been done on carbon isotopes and most often with CO_2 lasers.^{25–39} Carbon isotopic enrichment has been observed in single-wavelength, single-component reactants,^{25–27} multiple-wavelength (usually two or more CO_2 laser lines) conditions^{28–30} and in two-component, two-step processes.^{31–35} These studies have led to scale-up processes using two-step, two-component mixtures of carbon halides and halogen gases^{36–38} and multiple-pass single-component reaction conditions.³⁹

While the CO_2 laser frequencies are suitable for many MPD reactions, there are important fundamental vibrational frequencies such as the OH and C–H stretch in the $2.5\text{--}3.5 \mu\text{m}$ regions and C=O stretch in the $5.5\text{--}6.0 \mu\text{m}$ region which can be excited directly at these wavelengths. These frequency regions have been explored by using frequency-doubled CO_2 lasers,^{40,41} CO_2 ,^{42–44} HF,^{14,17,18,45} spin–flip Raman,⁴⁶ optical parametric oscillators,^{47–49} and others. Most of these sources have a limited tuning, range and exploration of wide regions of the vibrational spectrum relevant to MPD is not possible.

Free-electron lasers (FEL) are capable of tuning over the entire vibrational spectrum of interest to MPD with sufficient power to mediate dissociation.^{50–52} Recently, the FELs at Los Alamos and The Netherlands have been used for MPD of Freons in the $11\text{--}12 \mu\text{m}$ range but no isotope effects were reported.^{53–55} We have successfully used the Mark III infrared FEL at Duke University to achieve MPD of $\text{CH}_3\text{CH}_2\text{Cl}$ and CHClF_2 in the C–H stretch region⁵⁶ and now report on MPD of formic acid and carbon and oxygen isotopic selectivity in the C=O stretch region.

While MPD in formic acid has been observed at H–F laser frequencies^{17,45} and H/ ^2H isotopic selectivity has been reported,¹⁷

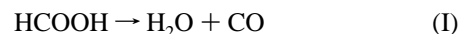
this is the first report on formic acid dissociation at the C=O stretch region and the first report on $^{12}\text{C}/^{13}\text{C}$ selectivity of MPD for formic acid.

Experimental Section

Experiments have been performed using an FEL, the Mark III, at Duke University.⁵² Its radiation can be tuned in the spectral range $2\text{--}9 \mu\text{m}$ s, ($1100\text{--}5000 \text{cm}^{-1}$), spectral width $\delta\lambda/\lambda$ being $0.01\text{--}0.02$. The temporal structure of laser radiation consists of macropulses (repetition rate 10 Hz; duration $2\text{--}4 \mu\text{s}$; energy $10\text{--}30 \text{mJ}$), each pulse being a sequence of micropulses (duration $1\text{--}2 \text{ps}$, repetition period 350ps). A cylindrical pyrex glass cell with 10cm length and 2cm i.d. with BaF_2 windows was constructed. The laser beam was focused inside the gas cell by BaF_2 lenses. The focal length of the lenses was varied within the range $10\text{--}200 \text{cm}$. A manometer, MKS Baratron type 122B (range of measurements $0\text{--}10 \text{Torr}$), was directly connected with the cell. The output manometer signal was measured by a digital voltmeter and could be transferred into a computer. The cell had a finger for gas freezing. The finger was placed into a copper container, the temperature of which was measured by a copper–constantan thermocouple and then amplified and also could be transferred into a computer.

The cell was evacuated to pressures less than 10^{-3}Torr and then was filled by either formic acid vapor with a natural concentration of carbon isotopes or a mixture of equal amounts of formic acid molecules with both ^{12}C and ^{13}C isotopes.

The molecules of formic acid are adsorbed very strongly by the walls of the cell, which causes a permanent pressure decrease in the cell. This decrease during the experiments ($5\text{--}10 \text{min}$) was about $5\text{--}20\%$. Therefore, the method used (pressure rise due to MPD) in our previous experiments⁷ was not applicable to experiments with formic acid. In these experiments, a different method was used. It is known that the dissociation of formic acid molecules proceeds over two channels:^{57,58}



Therefore the reaction mixture was frozen at the temperature of liquid nitrogen after a certain time of irradiation. Two of

[⊗] Abstract published in *Advance ACS Abstracts*, September 1, 1997.

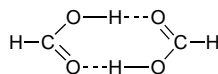
the possible products do not condense at liquid nitrogen, either CO or H₂, depending on the reaction channel. The pressure of the gas remaining after freezing the reaction mixture determined unambiguously the number of dissociated reactant molecules. The composition of products was determined with a mass spectrometer. The gas fraction that did not condense at -100 °C (CO, H₂, CO₂) was extracted for mass spectrometric analysis. The isotopic composition of products was determined by CO lines in mass spectrum.

Two sources of HCOOH were used in our experiments: the first containing 15% water initially, which was subsequently distilled at a temperature of 40 °C and a pressure of 100 Torr, and the second containing 1% water, which was not further purified. We did not see any difference between reaction rates of these two sources of HCOOH. The HCOOH containing 99% of the ¹³C isotope was used in experiments with isotope-enriched mixtures.

IR absorption spectra were obtained with a FTIR spectrometer. Spectral resolution was 1 cm⁻¹.

Results and Discussion

IR Spectra of HCOOH. Formic acid molecules at room temperature and a pressure of several Torr are mostly found as dimers that have a cyclic structure:⁵⁹



Several vibrational frequencies and widths of absorption bands are significantly different between the monomer and dimer and can significantly affect the MPD. Therefore in this section we will analyze the absorption IR spectra of formic acid in the vapor phase.

In our experiments, the variation of the C=O stretch vibrational band of the absorption spectrum due to dimer formation is of the most interest. The corresponding regions of the IR spectra of the HCOOH absorption at different pressures are shown at the top of Figure 1. The vibrational frequencies of dimers and monomers are well-known.⁵⁹ The band at 1777 cm⁻¹ belongs to the spectrum of the monomer, and the band at 1742 cm⁻¹ belongs to that of the dimer. The dimer–monomer equilibrium is shifted toward the dimer with increasing pressure. Therefore, the dimer absorption band increases relative to the monomer absorption band that remains almost stable with pressure increase.

To obtain the separate IR absorption spectra for monomer and dimer, we can use two methods. One of them is to calculate the concentration of dimers and monomers using the equilibrium constant. But a more accurate and direct way is to determine the linear combinations of experimental spectra that contain only the absorption bands at either 1777 or 1742 cm⁻¹. We chose the second method.

To determine the IR absorption spectra for monomer and that for dimer separately we used the spectra of formic acid obtained at two different pressures at room temperature. The linear combinations of such spectra that contain only the absorption bands at either 1742 or 1777 cm⁻¹ can be obtained. The spectra obtained at pressures of 1 and 5 Torr were used for this purpose. Thus, we have two linear equations:

$$S_d(\nu) = Sp(5, \nu) - FSp(1, \nu)$$

$$S_m(\nu) = Sp(1, \nu) - GSp(5, \nu)$$

where $S_d(\nu)$ and $S_m(\nu)$ are respectively the spectra of dimer

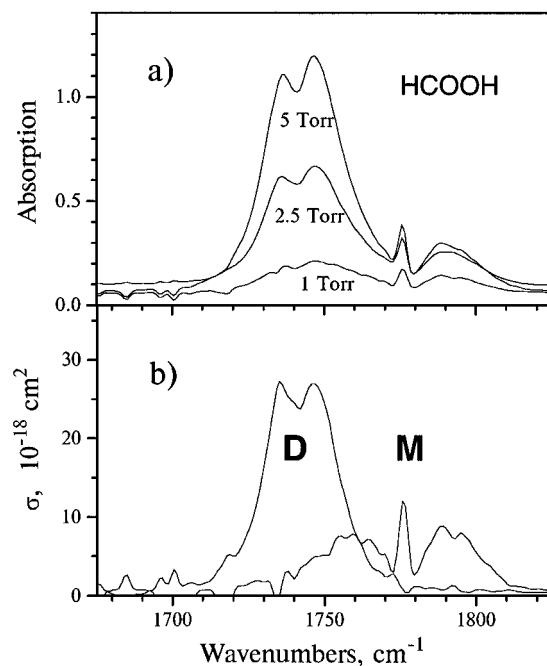


Figure 1. (a) Region of the IR absorption spectra for HCOOH measured at pressures of 1, 2.5, and 5 Torr. The fraction of dimer rises with increasing the total pressure. It is indicated by the relative increase of the spectral band at 1742 cm⁻¹. The separate spectra of dimers and monomers were obtained by linear combination of the spectra at different pressures. (b) Absorption coefficients in the same spectral region of the dimers (D) and the monomers (M) of formic acid.

and monomer, $Sp(5, \nu)$ and $Sp(1, \nu)$ are experimental spectra obtained at pressures of 5 and 1 Torr, and F and G are numerical coefficients.

The values $F = 2.7 \pm 0.3$ and $G = 0.108 \pm 0.018$ were obtained from the experimental spectra. The F coefficient is the ratio of the monomer concentration at pressures 5 and 1 Torr. G is the corresponding ratio for dimers. These coefficients can also be calculated using the constant for dimer–monomer equilibrium. This constant was obtained using experimental data reported in the literature.⁵⁹ It was found to be 0.45 Torr⁻¹. The calculations using this constant give $F = 3.21$ and $G = 0.098$, which agree satisfactorily with our present results.

The corresponding spectra of dimer and monomer separately are shown at the bottom of Figure 1. The coefficient of absorption is indicated as 10⁻¹⁸ cm²/molecule. The monomer absorption band has rotational P, Q, and R branches. The Q branch of the dimer absorption band was not observed. The total width of the dimer absorption band is found to be less than that of the monomer, which is expected, because the rotational constants for dimer molecules are less than those for monomer molecules.

We have also calculated the integral absorption coefficients for different absorption bands of the dimer and the monomer. The integral coefficient is

$$I = \int \sigma(\nu) d\nu$$

where σ is the absorption coefficient (cm²/molecule) and ν is the wavenumber (cm⁻¹). The results are presented in the second column of Table 1. Using the experimentally obtained integral intensities, we calculated transition dipole moments for some vibrations of the molecules. The results of the calculations are given in the fourth column of Table 1.

The integral intensities of the absorption band reported in the literature⁵⁹ are given in this table as well. (In that reference

TABLE 1

vibrational frequency, cm^{-1}	f^a cm	$I(\text{theory})$		$ M_{0-1} $, Q , cm
		km/mol	cm	
monomer				
2942	8.80×10^{-18}	53	8.80×10^{-18}	1.20×10^{-29}
1777	4.61×10^{-17}	533	8.85×10^{-17}	3.04×10^{-29}
dimer				
2957		156		
1742	7.31×10^{-17}	1188	19.7×10^{-17}	4.36×10^{-29}
1365	5.49×10^{-18}	75	12.4×10^{-18}	1.35×10^{-29}
1218	4.1×10^{-17}	478	7.9×10^{-17}	3.90×10^{-29}

^a This work.

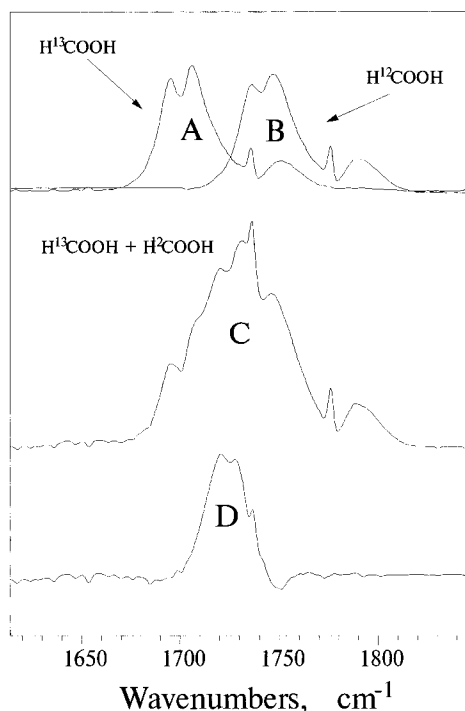


Figure 2. Procedure of extracting the absorption band of the C=O stretch vibrations of the mixed ^{12}C – ^{13}C dimer of the formic acid: (A) and (B) the spectra of the pure isotopic species obtained separately; (C) the spectrum of the isotopic mixture $\text{H}^{13}\text{COOH} + \text{H}^{12}\text{COOH}$ (50% + 50%), in which the mixed dimers are present as well as the pure ^{12}C – ^{12}C and ^{13}C – ^{13}C dimers; (D) the result of subtraction from spectrum C of the spectra A and B.

the integral intensities are measured in kilometers per mole without any definition of these units. We transferred these units into centimeters by dividing by 6.02×10^{18} .) The comparison of experimental and theoretical values shows that the experimental values are found 2–2.5 times lower than the theoretical ones. On the other hand, the relative intensities of different bands obtained from our experiments agree well with those of the theory except for the monomer band at 2942 cm^{-1} .

The IR absorption spectra of [^{13}C]formic acid were obtained. The region of spectrum containing the absorption band of the C=O stretch vibration is shown at the top of the Figure 2, curve A. The substitution of the isotope decreases the frequency of the C=O stretch vibration from 1777 to 1737 cm^{-1} in the monomer. In the dimer, the corresponding isomer shift is from 1742 to 1701 cm^{-1} . This is true only for the pure species containing either ^{12}C or ^{13}C . The mixed ^{12}C – ^{13}C dimers are present in a mixture of both isotopic species of formic acid molecules. We obtained the spectra of the mixed dimers of formic acid molecules in the region of absorption of the C=O stretch vibration. Such a spectrum obtained from a mixture of equal concentrations of formic acid of each isotope is shown

TABLE 2: Frequencies (cm^{-1}) of the Dimer C=O Stretch

dimer	this work	literature data
^{12}C – ^{12}C	1742	1754^{15} 1740^{16}
^{13}C – ^{13}C	1701	no data
^{12}C – ^{13}C	1725	no data

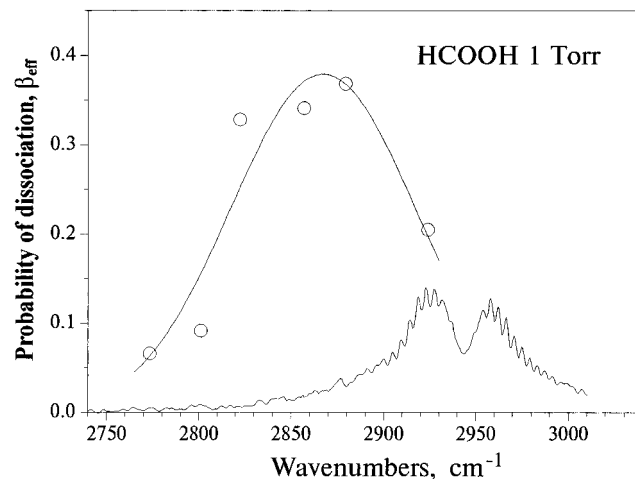


Figure 3. MPD spectrum of formic acid when the C–H stretch vibrations are being excited. The C–H stretch vibrational band of the ordinary IR absorption spectrum of the monomer is shown for comparison.

in Figure 2, curve C. This spectrum has a new feature at 1725 cm^{-1} , which is not present in the spectra of separate pure H^{12}COOH and H^{13}COOH . The spectrum of the mixture consists of five components: two bands corresponding to ^{12}C and ^{13}C monomers, two bands corresponding to ^{12}C – ^{12}C and ^{13}C – ^{13}C dimers, and one band corresponding to the mixed ^{12}C – ^{13}C dimer. The spectra of the pure components consist of just two components: monomer and dimer bands. We derived the separate spectrum of the mixed dimer by subtraction of the spectra of pure components multiplied by selected coefficients from the spectrum of the mixture (Figure 2, curve D). The coefficients were chosen to eliminate the features at 1777 and 1701 cm^{-1} . The features at 1742 and 1737 cm^{-1} did not disappear totally.

Table 2 presents the obtained frequencies of the dimer C=O stretch vibrations active in IR. We determined the frequencies in the spectrum of dimers as the center between P- and R-rotational bands. The accuracy of the determination is about 2 cm^{-1} .

MPD of Formic Acid at 3.5 and 5.5 μm . The MPD of formic acid at C–H stretch vibrational excitation was observed at sufficiently high energy fluences to cause a reaction. The experiments were mostly done with lens $f = 50 \text{ cm}$. The energy fluence at the focal point was 180 J/cm^2 , when the laser macropulse energy was 28 mJ . The dissociation probability dependence on the laser radiation wavenumber is shown in Figure 3.

As a measure of the probability, β_{eff} was used from the following equation:

$$\beta_{\text{eff}} = \frac{\Delta N}{nV_f} = \frac{\Delta N}{2\pi a \omega^2 h}$$

where ΔN is the number of molecules dissociated in one macropulse, n is the concentration, V_f is the volume of region close to the focal point, ω is the beam radius at the focal point, and a is the Rayleigh range.

The β_{eff} value is the probability of dissociation per one macropulse averaged over the volume near the focal point. The

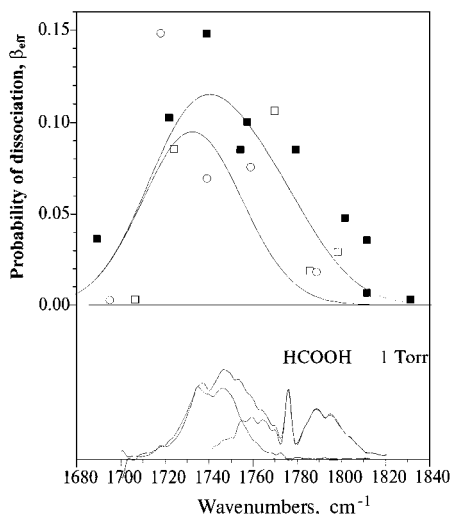


Figure 4. MPD spectrum of formic acid when the C=O stretch vibrations are being excited. It is deconvoluted into action spectra corresponding to the monomer and dimer excitation. The C=O stretch vibrational band of the ordinary IR absorption spectrum is shown as well. This band is also deconvoluted into the band of the dimer and the band of the monomer. Three types of symbols indicate the results of three different experiments in which the bandwidth of the FEL is different for each experiment.

relationship between β_{eff} and the true dissociation probability was reported in our previous publication.⁵⁶ The C–H stretch vibrational absorption band of formic acid is also shown in Figure 3. The maximum MPD yield is observed at wavenumbers significantly less than C–H stretch vibrational frequency. The value of the “red shift” was found to be about 70 cm^{-1} .

Upon exciting formic acid molecules at the C=O stretch vibrational band we observed the MPD taking place at significantly lower energy fluences than the MPD at C–H band excitation. Although the macropulse energy was $8\text{--}12 \text{ mJ}$ in the region $5.7\text{--}6.0 \mu\text{m}$, the energy fluences needed for the MPD in this region were easily obtained with the 90 cm focal length lens. The results of three different experiments, in which the MPD action spectrum was measured at a pressure of 1 Torr , are shown in Figure 4. A wide variation of the experimental values is associated with a large instability in the spectral content of the laser radiation in this region. The width reached 40 cm^{-1} in one of the experiments, and the spectral shape of the radiation was notched by the atmospheric absorption. The results of this experiment are shown as black filled squares in the figure. The widest MPD spectrum was obtained in this experiment compared with the two others, shown by squares and circles.

The averaged shape of the MPD spectrum in the region of the C=O stretch vibrational absorption can be represented by a wide asymmetric profile. At the bottom of the Figure 4 is shown the ordinary IR absorption spectrum in the region of C=O stretch vibration of the formic acid molecules at 1 Torr pressure. Decomposition of the IR spectrum to the monomer and dimer components is shown as well. We assumed the MPD spectrum to consist of two—monomer and dimer—components like the ordinary IR spectrum. To make this decomposition, we assumed the profile of each component to be Gaussian:

$$\beta_{\text{eff}}(\nu) = A \exp(-(\nu - \nu_{\text{mon}} - \rho)^2/\delta^2) + B \exp(-(\nu - \nu_{\text{dim}} - \rho)^2/\delta^2) \quad (1)$$

where $\nu_{\text{mon}} = 1777 \text{ cm}^{-1}$, $\nu_{\text{dim}} = 1737 \text{ cm}^{-1}$, A and B are the amplitudes of corresponding components, ρ is the shift of a component, and δ is the half-width of a component.

Choosing function 1, we have made the following assumptions: (a) The maximum of each component in the MPD spectrum is shifted by the same value from the maximum of the corresponding component of the ordinary IR spectrum (i.e., the monomer and dimer components both have the same red shift). (b) The component widths in the MPD spectrum are equal.

The last assumption is justified since the component width in the MPD spectrum is mostly determined by the laser radiation width. Thus, function 1 consists of only the four adjustable parameters.

The results of such calculations, the separate components of the MPD spectra, are shown in Figure 4. We obtained $\delta = 32 \text{ cm}^{-1}$ for the half-width of each component and $\rho = 10 \text{ cm}^{-1}$ for the “red shift”, and the ratio of the amplitudes of the components is $B/A = 1.79$.

The comparison of the MPD probabilities at excitation in the different spectral regions is of some interest. Special experiments were carried out to decrease the errors of the comparison. First, the “effective probability” of dissociation β_{eff} was determined at excitation in the $3.6 \mu\text{m}$ region with a lens of 90 cm focal length. Then, under the same experimental conditions, the macropulse energy was adjusted to the value at which β_{eff} at excitation at $5.7 \mu\text{m}$ was equal to that at $3.6 \mu\text{m}$ excitation. The equal probabilities were obtained when the energy fluence at $3.6 \mu\text{m}$ was 16 times more than that at $5.7 \mu\text{m}$, thus, for $3.6 \mu\text{m}$ 56 J/cm^2 and for $5.7 \mu\text{m}$ 3.4 J/cm^2 .

The transition dipole moment $M_{0 \rightarrow 1}$ for the C=O stretch vibration is 2.53 times more than that for the C–H stretch vibration of formic acid molecules. The value of the interaction of molecules with the laser radiation is proportional to $(M_{0 \rightarrow 1}E)$, where E is the electric field in the radiation wave. The energy fluence is proportional to E^2 ; therefore, the interaction of the C–H vibration with the laser radiation becomes equal to that of the C=O vibration when the ratio of the corresponding energy fluences is $2.53^2 = 6.4$. The energy of the quantum of the C–H vibrational mode is more than that of the C=O vibrational mode; therefore, the ratio of energy fluences required for equal reaction rates is expected to be less than 6.4. Actually this ratio obtained from experiment is about 16.

The excitation of the C=O stretch vibrations is found to be significantly more effective for the MPD of formic acid than the excitation of the C–H stretch vibrations of formic acid. This difference cannot be explained by the different intensities of the corresponding absorption bands in the IR spectrum of the formic acid molecule. Perhaps it could be associated with some details of interaction of the different vibrations in the strongly excited molecule. For example, we observed a large red shift in the MPD spectrum at the C–H stretch vibrational excitation (about 70 cm^{-1}). However at the C=O vibrational excitation, the red shift was 10 cm^{-1} . The C–H/stretch mode of formic acid is much like that in CHClF_2 . There is a large anharmonicity which cannot be compensated by rotational excitation mechanisms. In addition, there are no nearly degenerate C–H modes into which to couple energy and the excitation in the first two levels must be accomplished with very little help from the usual molecular compensation mechanisms.

The pressure dependence of the MPD probability β_{eff} is shown in Figure 5. The probability decreases with increasing pressure due to collisional deactivation. The shape of this dependence is quite different from that reported by other authors.⁴⁵ These authors found the probability to be proportional to pressure. This fact indicates that the MPD in our experiments does not need collisions between excited molecules unlike in the experiments⁴⁵ in which the dissociation requires collisions.

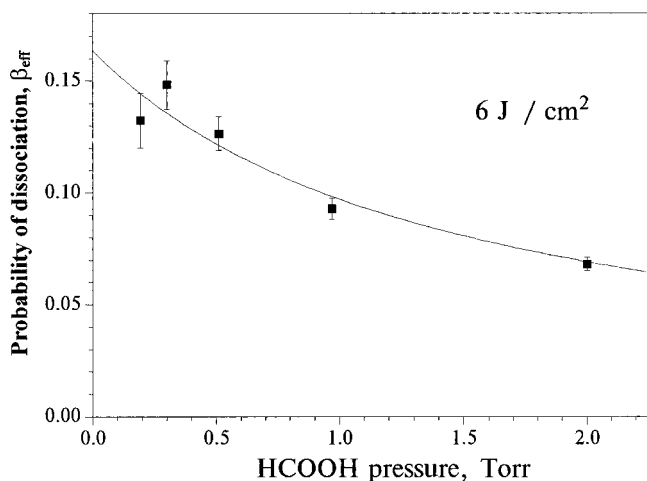
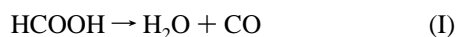


Figure 5. Pressure dependence of the HCOOH dissociation probability at C=O stretch vibrational mode excitation.

MPD Products. The dissociation of formic acid can follow two channels:



Different methods have been used to study the thermal decomposition of formic acid. HCOOH decomposition has been investigated in a static reactor,^{61,62} in a flow system,⁵⁷ by laser heating,⁵⁸ and in shock tubes.^{63,64} The serious drawback of some of these experiments is the effect of the walls of reaction volume. The methods of laser heating and shock tubes do not have this drawback; therefore, the most reliable information about the decay channels and the rate constants of decay have been obtained using these methods.^{58,63,64} The main products of thermal decomposition of HCOOH are CO and H₂O. The content of CO₂ did not exceed 10⁻¹² and 2%.⁶⁴ The reason for the small content of CO₂ is that the threshold of dissociation by channel II is higher than that by channel I. For the decay of HCOOH to CO and H₂O, the threshold value is given as 66 ± 4 ⁵⁸ and 63 ± 2 kcal/mol.⁶³ For the decay to CO₂ and H₂, the threshold is estimated as 67 ± 2 kcal/mol.⁶³ Unfortunately, the results reported in the literature⁶³ do not allow us to determine the ratio of pre-exponential factors for the monomolecular decay by these two channels, because the experiments have been done at the lower pressure limit. The quantum chemical calculations predict a large difference between thresholds of these two channels, values of which are obtained as 62 and 81 kcal/mol for channels I and II, respectively.⁶⁴ Therefore, the second reaction (decarboxylation) usually takes place only on the surface, i.e., catalytically.⁶⁵

Based on literature data, the main channel of MPD of HCOOH is expected to be channel I. However, channel II could be expected at high density of the laser radiation. The analysis of the dissociation products unfrozen at -100 °C indicated that CO is the main product of our experiments. The CO₂ amount was about 2% compared to CO when determined by mass spectrometer analysis and by measuring the temperature dependence of the vapor pressure. Unfortunately, we were not able to determine the amount of H₂ because of a large and unreproducible background at the line $m/e = 2$. The fact that the amounts of CO₂ were found equal in experiments with lenses of 50 and 100 cm focal lengths was not expected. This observation may be explained by the fact that, although the energy fluence is 4 times more at the focal point with the 50 cm focal length lens than that with the 100 cm focal length

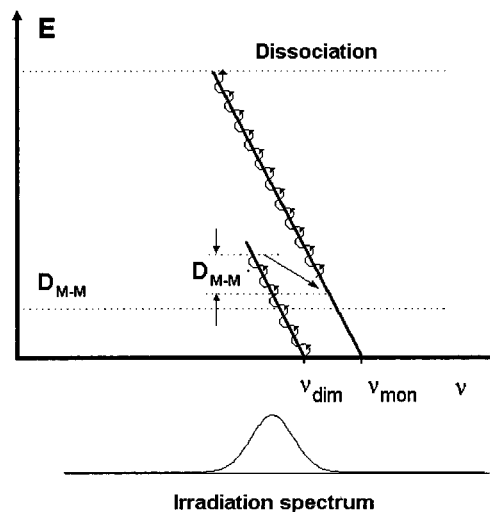


Figure 6. Proposed sequence of the steps that occurs during the multiphoton excitation of formic acid by irradiation tuned to the spectral region of the dimer absorption band C=O stretch vibrational mode. The spectrum of irradiation is shown at the bottom. The dimer and monomer absorption bands are shifting toward the red with increasing energy absorbed by the molecule due to anharmonicity. This shift hinders the further excitation of the irradiated molecule. The dimers absorb at a frequency lower than the monomers. Excitation of the molecular system starts as excitation of the dimer. After the dimer is dissociated this excitation is continued as the monomer's excitation. When the dimer is dissociated, the absorption band of the molecular system shifts toward the blue and this shift makes the further excitation of the molecular system easier. D_{M-M} is the bond energy of two monomer molecules in dimer.

lens, the products are mostly created in the volume far from the focus where channel II is predominant.

Role of Dimers in MPD of Formic Acid. From our experiments, we can conclude that the excitation of dimers is more effective for MPD than the excitation of monomers. Actually, the vapor of HCOOH at room temperature and a pressure of 1 Torr contains 25% dimers and 75% monomers. As follows from Figure 4, the ratio between dimer and monomer contributions in the MPD spectrum is 1.79:1. Therefore, when dimers are excited, the yield of products will be 5.37 times more than for monomer excitation, or 2.68 times more taking account that the number of atoms in the dimer is twice the number of atoms in the monomer. This conclusion is based on the deconvolution of the MPD spectra and is therefore not certain. But the estimations done above show that the role of dimers in HCOOH MPD should be examined further.

Two stages are commonly distinguished in the process of multiphoton excitation with infrared laser radiation. The first stage is excitation in the region of discrete vibrational levels, the second, in the region of vibrational quasicontinuum.^{1,2,5} The main problem at the first stage is to compensate the anharmonicity. There are a number of mechanisms proposed for anharmonicity compensation in the literature. For example, rotational excitation (the P-Q-R mechanism),^{6,8,66,67} anharmonic splitting of degenerate vibrational levels,^{48,49} multiquanta excitation,⁶⁸ and power broadening,^{69,71} have been postulated to be important in MPD.

In addition, another mechanism for the anharmonicity compensation can be considered - the mechanism based on the fact that the frequency of the C=O stretch vibrations in the dimer is less than that in the monomer. The proposed sequence of the steps that occur during the multiphoton excitation of the formic acid molecule by the irradiation tuned in the spectral region of the dimer absorption band (C=O stretch vibrational mode) is shown in Figure 6. The spectrum of the irradiation

pulse is shown at the bottom. The dimer and monomer absorption bands are shifting toward the red with increasing energy of the molecule due to anharmonicity. This shift hinders the further excitation of the irradiated molecule. The dimers absorb at a frequency lower than the monomers. Excitation of the molecular system starts as excitation of the dimer. After the dimer is dissociated into two monomers, this excitation is continued as monomer excitation. When the dimer is dissociated, the absorption band of the molecular system shifts toward the blue and this shift makes the further excitation of the molecular system easier.

Such a mechanism of anharmonicity compensation requires that the amount of energy absorbed by the dimer is sufficient for dissociation of the dimer and excitation of at least one of its monomers. The dissociation energy of formic acid dimers varies from 12 to 15 kcal/mol.¹³ For the dimer having absorbed 4, 5, 6, and 7 quanta of irradiation, calculations using RRKM theory predict that the lifetimes will be 5, 0.7, 0.23, and 0.1 ns, respectively. In our experiments, the excitation takes place during the macropulse of 2–3 μ s. Such short life times as predicted by RRKM mean that the excitation of the dimer to energies sufficient for dissociation into products ($\text{H}_2\text{O} + \text{CO}$) is not possible. However, it is not clear how accurate the lifetime estimations using the RRKM theory are at such low energies.

All these estimations show that the question about the comparative efficiency of MPD when dimers or monomers are being excited is not yet understood and direct experimental measurements are needed.

Carbon Isotope-Selective MPD of HCOOH. These experiments were performed with the mixture $\text{H}^{12}\text{COOH} + \text{H}^{13}\text{COOH}$ (50% + 50%). The reaction mixture after irradiation by the FEL was frozen with liquid nitrogen. The remaining gas after freezing, CO, was analyzed by mass spectrometer. The isotopic composition of CO depended on the irradiation wavelength. The results of experiments carried out at 1 Torr pressure are shown at the top of Figure 7. Maximum of selectivity which is determined as a ratio of rate constants of dissociation of the chosen isotope to the remaining isotope, was 23 for ^{12}C as the chosen isotope and 3 for ^{13}C as the chosen isotope. The dissociation yield was about 20% in these experiments.

On the basis of the MPD spectra of the isotopic components of our mixture, we can calculate the maximal possible selectivity as a function of wavenumber of the laser radiation. In HCOOH mixtures, the calculations become more complicated because of the dimers. In the mixture of H^{12}COOH and H^{13}COOH , five components are actually present: H^{12}COOH (^{12}C monomers), H^{13}COOH (^{13}C -monomers), $(\text{H}^{12}\text{COOH})_2$ ($^{12}\text{C}-^{12}\text{C}$ dimers), $(\text{H}^{13}\text{COOH})_2$ ($^{13}\text{C}-^{13}\text{C}$ dimers) and $\text{H}^{12}\text{COOH}-\text{H}^{13}\text{COOH}$ ($^{12}\text{C}-^{13}\text{C}$ dimers). Since the constant for the dimer–monomer equilibrium is not changed on replacing the carbon isotopes, the total numbers of monomers and dimers are the same in our isotopic mixture at 1 Torr pressure as in the ordinary formic acid at 1 Torr pressure. Then we can deconvolute the MPD spectrum of our mixture into two Gaussian components corresponding to the monomer and dimer contributions. We can also decompose the Gaussian of the monomers to two Gaussian components corresponding to ^{12}C monomers and ^{13}C monomers with ratio of the intensities 1:1. We have decomposed The Gaussian of the dimers to three Gaussian components corresponding to the three types of dimers present in our mixture. The ratio of intensities for the three Gaussians is 1:2:1. As a result, we obtain the contributions of different components of our mixture to the MPD spectrum of the mixture. These contributions are shown at the bottom of Figure 7.

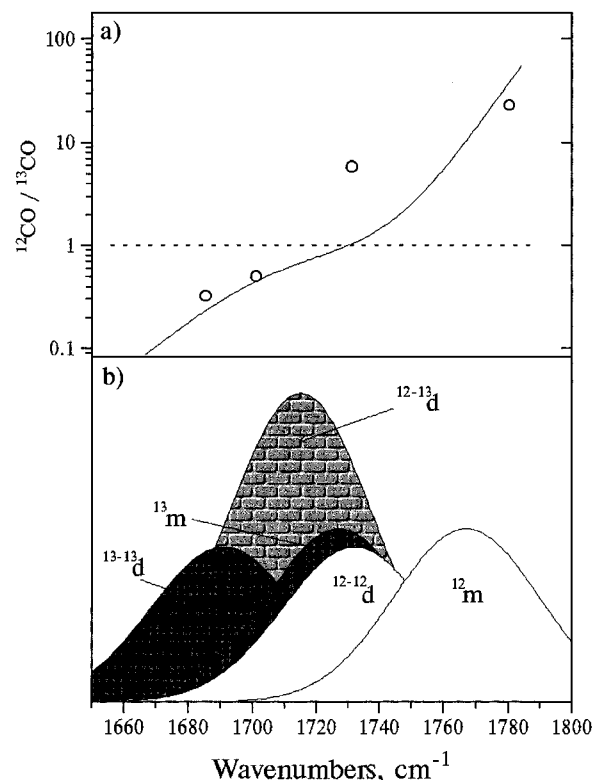


Figure 7. (a) Dependence of the isotopic selectivity on the irradiation wavenumber for the isotopic mixture $\text{H}^{12}\text{COOH} + \text{H}^{13}\text{COOH}$ (50% + 50%). Circles, experiment and solid line, simulations based on the MPD spectra; dashed line is the absence of selectivity. (b) The MPD spectra of different isotopic species of dimers and monomers of formic acid. The spectra are constructed based on the MPD spectra of ^{12}C monomers and $^{12}\text{C}-^{12}\text{C}$ dimers (Figure 4.).

When the ^{12}C monomers or $^{12}\text{C}-^{12}\text{C}$ dimers are dissociated, ^{12}CO is created. When the ^{13}C monomers or $^{13}\text{C}-^{13}\text{C}$ dimers are dissociated, ^{13}CO is created. We considered as the simplest assumption that when the $^{12}\text{C}-^{13}\text{C}$ dimers are dissociated equal amounts of ^{12}CO and ^{13}CO are created. As a result, we have for the selectivity the following expression:

$$S(\nu) = [(A/2) \exp(-(\nu - 1767)^2/\delta^2) + (B/4) \exp(-(\nu - 1732)^2/\delta^2) + (B/2) \exp(-(\nu - 1715)^2/\delta^2)] / [(A/2) \exp(-(\nu - 1627)^2/\delta^2) + (B/4) \exp(-(\nu - 1691)^2/\delta^2) + (B/2) \exp(-(\nu - 1715)^2/\delta^2)] \quad (2)$$

The symbols used in (2) are the same as were used in (1). The values of the ^{12}C monomer, $^{12}\text{C}-^{12}\text{C}$ dimer, ^{13}C -monomer, $^{12}\text{C}-^{13}\text{C}$ dimer, and $^{13}\text{C}-^{13}\text{C}$ dimer frequencies substituted in (2) are decreased by the value of the red shift $\rho = 10 \text{ cm}^{-1}$. The half-width of each Gaussian δ is taken as 32 cm^{-1} , the amplitudes $A = 1$ and $B = 1.79$. The results are shown in Figure 7a with the solid line.

Comparison of the calculated values of selectivity with the values obtained in our experiments shows that at the edges of the spectral region of the MPD the experimental values are close to the maximum possible values determined by the ratio (2) of the MPD spectra. A discrepancy between the experimental and calculated values is observed in the middle of the spectral range. It is possible that upon dissociation the vibrationally excited ^{13}C species is shifted far enough into the red that it is no longer in resonance, while the vibrationally excited ^{12}C species is

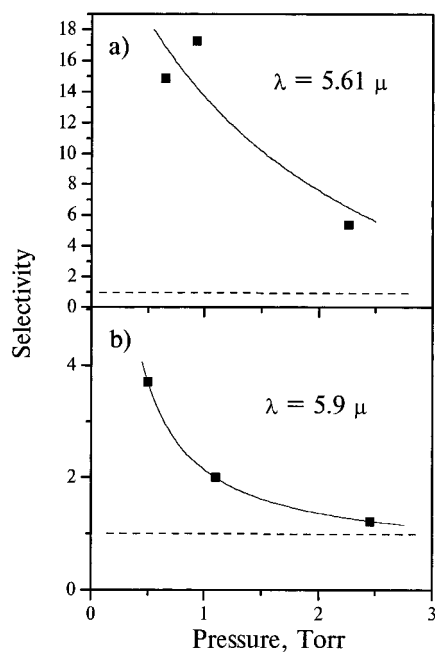


Figure 8. Pressure dependence of isotopic selectivity for the isotopic mixture $\text{H}^{12}\text{COOH} + \text{H}^{13}\text{COOH}$ (50% + 50%). (a) Excitation in the spectral region, in which the dimer absorption is small. (b) Excitation in the spectral region in which the dimer absorption is dominant.

shifted into better resonance. Since the dissociation of the mixed dimer can leave either the ^{12}C or the ^{13}C in the vibrationally excited state, the red shift may give isotopic selectivity to the ^{12}C molecules even though there may be a lower percentage of ^{12}C formic acid molecules excited upon dissociation.

The pressure dependence of the selectivity was measured at two irradiating wavenumbers of 1695 and 1780 cm^{-1} . The results of the measurements are shown in Figure 8. In both cases, the selectivity decreases with increasing pressure that is associated with a collisional exchange of excitation between the formic acid molecules of different isotopes. The selectivity decrease with increasing pressure is found to be faster at 1695 cm^{-1} , where the contribution of dimers to the MPD is large.

Carbon Isotope-Selective MPD of Formic Acid with Natural Isotopic Content. The natural content of ^{13}C is 1.1%. As a measure of the isotopic selectivity of the MPD process, the ratio of the rate constant for dissociation of formic acid molecules containing ^{13}C to the rate constant for dissociation of formic acid molecules containing ^{12}C was calculated from experiment. At small yields the selectivity can be determined as

$$S = \frac{[^{13}\text{CO}] 0.989}{[^{12}\text{CO}] 0.011} \quad (3)$$

The experiments were performed at a pressure of 0.7 and 0.5 Torr. The wavenumber of the laser radiation was chosen within the region 1690–1720 cm^{-1} . After 10–40 min of irradiation, the contents of the cell were frozen by liquid nitrogen. CO produced due to the MPD remained unfrozen and was analyzed by mass spectrometer. The isotopic effects were found to be unexpectedly high. In one of the first experiments, we observed the enrichment of CO products by ^{13}C isotope being 5.1% at a reaction yield of 24%. It is evident that in this experiment almost all the ^{13}C contained in the initial formic acid was transferred into the reaction product, CO. To measure a true selectivity, in the following experiments, MPD was performed to obtain a reaction yield not exceeding 2%. The

highest isotopic effect was 22. It was obtained at 0.5 Torr total pressure, and reaction yield was 1.5%.

The isotopic effect measured in the naturally occurring isotopic mixture was found to be higher than the isotopic effect in the 50% + 50% mixture of each isotopic species measured at the same wavelength of laser radiation. Based on the MPD spectra, we calculated the selectivity for the mixture of the natural carbon isotopic contents. The calculations were done using a formula similar to (2), in which the ratio of concentrations of the different isotopic types of the formic acid molecules was taken into account. The calculations predict an increase of the selectivity for the natural isotope-containing mixture; however, the experimental values of the selectivity are much higher than those calculated.

Selectivity increase in very dilute mixtures is known.⁷² It is associated with features of energy transfer between molecules in very dilute mixtures. But the isotopic effect in our experiments was found to be much higher than calculated from the MPD spectra. The reason for this is not clear. Let us only note that the spectrum of the laser radiation during the experiments with the natural isotopic content was quite complicated. It contained not less than two relatively narrow peaks, the width of each being 5–10 cm^{-1} .

In addition to enrichment with ^{13}C isotope, which was indicated by a mass spectral line of $m/e = 29$, we observed that the line $m/e = 30$ often increased in the mass spectra of products. The compound $^{12}\text{C}^{18}\text{O}$ corresponds to this line, and it is very plausible that the enrichment with ^{18}O was taking place parallel with that of ^{13}C . The natural content of the ^{18}O isotope is 0.2%. We observed the $m/e = 30$ line to be 1% of the $m/e = 28$ line; therefore, enrichment with ^{18}O isotope was increased 5 times.

Conclusion

In the experiments reported here, the infrared multiphoton dissociation of formic acid has been performed for the first time using radiation from the free electron laser. The large tunability of the FEL allowed a comparative study of MPD performed at the excitation of the C=O stretch vibrational mode of HCOOH as well as C–H stretch vibrational mode. We have been able to determine that initial excitation in the dimer is more efficient for MPD than is initial excitation of the monomer. We have also been able to obtain isotopic MPD with predominance of either the ^{12}C component or the ^{13}C component. The results show great potential of the molecular IR MPD at the C=O stretch vibrational excitation. The carbon isotope selectivity attained in our experiments with formic acid is comparable with the results on isotope-selective MPD of Freons performed with CO_2 lasers.

Acknowledgment. We are grateful to Dr. P. Y. Chen from the Chemistry Department of Duke University for obtaining the FTIR spectra of our compounds and A. Krasnopoler for mass spectrometric analysis. We thank Prof. Yu. Molin, ICK&C for helpful discussion. This work sponsored in part by the Medical Free Electron Laser Program, Office of Naval Research.

References and Notes

- (1) Ambartzumian, R. V.; Letokhov, V. S. In *Chemical and Biochemical Applications of Lasers*; Moore, C. B., Ed.; Academic Press: New York, 1977; Vol. 3, pp 167–316.
- (2) Lyman, J. L.; Quigley, G. P.; Judd, O. P. In *Multiple Photon Excitation and Dissociation of Polyatomic Molecules*; Cantrel, C. D., Ed.; Springer-Verlag: New York, 1986; pp 9–94.
- (3) Drouin M.; Gauthier M.; Pilon R.; Hackett P. A.; Willis C. *Chem. Phys. Lett.* **1978**, *60*, 16.
- (4) Lupo, D. W.; Quack, M. *Chem. Rev.* **1987**, *87*, 181.
- (5) Molin, Yu. N.; Panfilov, V. N.; Petrov, A. K. *Infrared Photochemistry*; Nauka: Novosibirsk, 1985 (in Russian).

- (6) Ambartsumyan, R. V.; Gorokhov, Yu. A.; Letokhov, V. S.; Marakov, G. N.; Puretskii, A. A. *Sov. Phys. JETP* **1976**, *44*, 231.
- (7) Lyman, J. L.; Hudson, J. W.; Freund, S. M. *Opt. Commun.* **1977**, *21*, 112.
- (8) Ambartsumyan, R. V.; Yu, A. G.; Letokhov, V. S.; Makarov, G. N.; Puretskii, A. A. *JETP Lett.* **1976**, *23*, 22.
- (9) Fuss, W.; Cotter, T. P. *Appl. Phys.* **1977**, *12*, 265.
- (10) Hackett, P. A.; Willis, C.; Gauthier, M. *J. Chem. Phys.* **1979**, *71*, 2682.
- (11) Majima, T.; Sugita, K.; Arai, S. *Chem. Phys. Lett.* **1989**, *163*, 29.
- (12) Lohman, V. N.; Marakov, G. N.; Ryabov, E. A.; Sotnikov, M. V. *Quantum Electron.* **1996**, *26*, 79.
- (13) Churakov, V.; Fuss, W. *Appl. Phys. B* **1996**, *62*, 203.
- (14) Laptev, V. B.; Ryabov, E. A.; Tumanova, L. M. *Quantum Electron.* **1995**, *22*, 607.
- (15) McAlpine, R. D.; Evans, D. K.; McClusky, F. K. *Chem. Phys.* **1979**, *39*, 263.
- (16) Ungureanu, C.; Almasan, V.; Ungureanu, M. *Infrared Phys. Technol.* **1996**, *37*, 451.
- (17) Takeuchi, K.; Inoue, I.; Nakane, R.; Makide, Y.; Kato, S.; Tominaga, T. *J. Chem. Phys.* **1982**, *76*, 391.
- (18) Evans, D. K.; McAlpine, R. D.; McClusky, F. K. *Chem. Phys.* **1978**, *32*, 81.
- (19) McAlpine, R. D.; Evans, D. K.; McClusky, F. K. *Chem. Phys.* **1979**, *39*, 263.
- (20) Fuss, W.; Schmid, W. E. *Ber. Bunsenges. Phys. Chem.* **1979**, *83*, 1148.
- (21) Zittel, P. F.; Darnton, L. A., and Little, D. D. *J. Chem. Phys.* **1983**, *79*, 5991.
- (22) Vizhin, V. V.; Molin, Yu. N.; Petrov, A. K.; Sorokin, A. R. *Appl. Phys.* **1978**, *17*, 385.
- (23) Marling, J. *J. Chem. Phys.* **1977**, *66*, 4200.
- (24) Abzianidze, T. G.; Baranov, V. Yu.; Bakhtadze, A. B.; Belykh, A. D.; Vetsko, V. M.; Gurashvili, V. A.; Egiazarov, A. S.; Lzyesmov, S. V.; Kuz'menko, V. A.; Oziashvili, E. D.; Ordzhonikidze, M. O.; Partskhaladze, G. Sh.; Petrov, A. K.; Pis'mennyi, V. D.; Pultillin, V. M.; Strel'tsov, A. P.; Tevzadse, G. A.; Khomenko, S. V. *Sov. J. Quantum Electron.* **1986**, *16*, 137.
- (25) Arai, S.; Kaetsu, H.; Isomura, S. *Appl. Phys.* **1991**, *B53*, 199.
- (26) Abdushelishvili, G. I.; Avatkov, O. N.; Bagratashvili, V. N.; Baranov, V. Yu.; Bakhtadze, A. B.; Velikhov, E. P.; Vetsko, V. M.; Gverdsiteli, I. G.; Dolzhikov, V. S.; Esadze, G. G.; Kazakov, S. A.; Kolomüskü, Yu. R.; Letokhov, V. S.; Pigul'skii, S. V.; Pis'mennyi, V. D.; Ryabov, E. A.; Tkeshelashvili, G. I. *Sov. J. Quantum Electron.* **1982**, *12*, 459.
- (27) Gauthier, M.; Cureton, C. G.; Hackett, P. A.; Willis, C. *Appl. Phys.* **1982**, *B 28*, 43.
- (28) Batra, A. Sarkar, S. K.; Parthasarathy, V. *J. Photochem. Photobiol.* **1994**, *A 83*, 193.
- (29) Evseev, A. V.; Letokhov, V. S.; Puretzky, A. A. *Appl. Phys.* **1985**, *B 36*, 93.
- (30) Evseev, A. V.; Laptev, V. B.; Pureskii, A. A.; Ryabov, E. A.; Furzikov, N. P. *Sov. J. Quantum Electron.* **1988**, *18*, 385.
- (31) Fuss, W.; Göthel, J.; Ivanenko, M.; Kompa, K. L.; Schmid, W. E. *Z. Phys.* **1992**, *D24*, 47.
- (32) Ma, P.; Sugita, K.; and Arai, S. *Appl. Phys.* **1990**, *B51*, 103.
- (33) Ma, P. H.; Sugita, K.; and Arai, S. *Appl. Phys.* **1990**, *B50*, 385.
- (34) Ma, P. H.; Sugita, K.; and Arai, S. *Appl. Phys.* **1989**, *B49*, 503.
- (35) Arai, S.; Sugita, K.; Ma, P.; Ishikawa, Y.; Kaetsu, H.; and Isomura, S. *Appl. Phys.* **1989**, *B48*, 427.
- (36) Ma, P.; Sugita, K.; Arai, S. *Chem. Phys. Lett.* **1987**, *137*, 590.
- (37) Sugita, K.; Ma, P.; Ishikawa, Y.; Arai, S. *Appl. Phys.* **1991**, *B52*, 266.
- (38) Chen, G. C.; Wu, B.; Liu, J. L.; Jing, Y.; Chu, M. X.; Xue, L. L.; Ma, P. H. *Appl. Phys.* **1995**, *B60*, 583.
- (39) Outhouse, A.; Lawrence, P.; Gauthier, M.; Hackett, P. A. *Appl. Phys.* **1985**, *B36*, 63.
- (40) Fuss, W.; Göthel, J.; Ivanenko, M. M.; Kompa, K. L.; Schmid, W. E.; Witte, K. *Z. Phys.* **1994**, *D29*, 291.
- (41) Truskin, S. A.; Sugawara, K.; Takeo, H. *Chem. Phys. Lett.* **1995**, *236*, 402.
- (42) Laptev, V. B.; Ryabov, E. A.; Tumanova, L. M. *Quantum Electron.* **1995**, *22*, 607.
- (43) Poliakov, M.; Davies, B.; McNeish, A.; Tranquille, M.; Turner, J. *Ber. Bunsenges. Phys. Chem.* **1978**, *82*, 121.
- (44) McNeish, A.; Poliakov, M.; Smith, K. P.; Turner, J. *J. Chem. Soc., Chem. Commun.* **1976**, 859.
- (45) Ding, H. B.; Shen, Z. Y.; Zhang, C. H. *SPIE Proc.* **1993**, *1859*, 234.
- (46) Corkum, R.; Willis, C.; Back, R. A. *Chem. Phys.* **1977**, *24*, 13.
- (47) Poliakov, M.; Breedon, N.; Davies, B.; McNeish, A.; Turner, J. *J. Chem. Phys. Lett.* **1978**, *56*, 474.
- (48) Hall, R. B.; Kaldor, A. *J. Chem. Phys.* **1979**, *70*, 4027.
- (49) Dai, H. L.; Kung, A. H.; Moore, C. B. *J. Chem. Phys.* **1980**, *73*, 6124.
- (50) Dai, H. L.; Kung, A. H.; Moore, C. B. *Phys. Rev. Lett.* **1979**, *43*, 761.
- (51) Brau, C. A. *Free Electron Lasers*; Academic Press: Boston, MA, 1990.
- (52) Benson, S. V.; Fann, W. S.; Hooper, B. A.; Madey, J. M. J.; Szarmes, E. B.; Richman, B.; Vintro, L. *Nucl. Instrum. Methods Phys. Res. A* **1990**, *296*, 110.
- (53) Marshall, T. C. *Free Electron Lasers*; MacMillan: New York, 1985.
- (54) Newnam, B. E.; Early, J. W.; Lyman, J. L. *Nucl. Instrum. Methods Phys. Res.* **1994**, *A341*, 142.
- (55) Newnam, B. E.; Lyman, J. L.; Early, J. W.; Van der Meer, A. F. *G. First International FEL User's Workshop*; Stanford, CT, 1994; p 15.
- (56) Lyman, J. L.; Newman, B. E.; Early, J. W. *J. Phys. Chem.* **1997**, *A101*, 49.
- (57) Petrov, A. K.; Chesnokov, E. N.; Gorelik, S. R.; Straub, K. D.; Szarmes, E. B.; Madey, J. M. J., submitted for publication in *J. Phys. Chem.*
- (58) Blake, P. G.; Davies, H. H.; Jackson, G. E. *J. Chem. Soc. B* **1971**, *10*, 1923.
- (59) Samsonov, Yu. N.; Petrov, A. K.; Baklanov, A. V.; Vizhin, V. V. *React. Kinet. Catal. Lett.* **1976**, *5*, 197.
- (60) Chang, Y. T.; Yamaguchi, Y.; Miller, W. H.; Schaefer, H. F., III *J. Am. Chem. Soc.* **1987**, *109*, 7245.
- (61) Demtredor, V. *Laser Spectroscopy. Basic Principles And Experimental Technics*; Nauka: Moscow, 1985 (in Russian).
- (62) Blake, P. G.; Jackson, G. E. *J. Chem. Soc. B* **1960**, *J*, 94.
- (63) Blake, P. G.; Hinshelwood, C. *Proc. R. Soc. Ser.* **1960**, *A255*, 444.
- (64) Hsu, D. S. Y.; Shaub, W. M.; Blackburn, M.; Lin, M. C. The Nineteenth International Symposium on Combustion, The Combustion Institute: Pittsburgh, 1983.
- (65) Saito, K.; Kakumoto, T.; Kuroda, H.; Torii, S.; Imamura, A. *J. Chem. Phys.* **1984**, *80*, 4989.
- (66) Petrov, A. K.; Balakina, G. G. *Commun. Siberian Branch A. Sci. USSR* **1970**, *N1*, 160. (In Russian).
- (67) Ackerhalt, J. R.; Galbraith, H. W. *J. Chem. Phys.* **1978**, *69*, 1200.
- (68) Horsley, J. A.; Stone, J.; Goodman, M. F.; Dows, D. A. *Chem. Phys. Lett.* **1979**, *66*, 461.
- (69) Brenner, D. M.; Spencer, M.; Steinfeld, J. I. *J. Chem. Phys.* **1981**, *75*, 3153.
- (70) Horsley, J. A.; Stone, J.; Goodman, M. F.; Dows, D. A. *Chem. Phys.* **1976**, *65*, 5062.
- (71) Bloembergen, N. *Opt. Commun.* **1975**, *15*, 416.
- (72) Jang, J. C.; Setser, D. W.; Danen, W. C. *J. Am. Chem. Soc.* **1982**, *104*, 5440.
- (73) Bagratashvili, V. N.; Dolgikov, V. S.; Letokhov, V. S.; Riabov, E. A. *Lett. JETP*, **1978**, *4*, 1181 (in Russian).